A Deformable Surface Model on the basis of the Theory of a Cosserat Surface

Wu Shin-Ting
Electrical and Computer Engineering Faculty
State University of Campinas
P.O.Box 6101 13083-970
Campinas, SP - Brazil
ting@dca.fee.unicamp.br

Vanio Fragoso de Melo
Departament of Mathematics and Statistics
Federal University of Campina Grande
P.O.Box 10044 58109-970
Campina Grande, PB - Brazil
vanio@dme.ufcg.edu.br

Abstract

This paper aims at proposing an elastically deformable surface with use of differential geometric structures. On the basis of the Theory of a Cosserat Surface, a computationally processable equation that relates the accumulated elastic energy and the variations in the differential geometry variables (metric and curvature tensors) of the deformable surface is presented. On the basis of our analysis, we propose a novel algorithm to compute more precisely, without compromising the interface's simplicity, the potential deformation energy in terms of the derivatives of the surface. With our proposal, we may maintain the finite difference scheme for computing deformations iteratively. Some simulation results are included.

1. Introduction

Deformable surface modeling techniques have been proposed either for support garment engineering or for entertainment and advertising purposes. They range from pure geometrical models, such as the pioneering work by Weil [15], to the models based on different shell theories, such as the fabric models proposed by Chen and Govindaraj [4], Eischen et al. [6] and Au et al. [1].

Using the fact that the energy stored in a deformable model was the sum of the energy due to stretching, bending, and the work done by the external forces, Terzopoulos et al. [14] developed a deformable surface model which relates the Lagrangian motion equation with the intrinsic geometry of the deforming surface

$$\mu\frac{\partial^2\mathbf{r}}{\partial t^2}+\gamma\frac{\partial\mathbf{r}}{\partial t}+\frac{\delta\varepsilon(\mathbf{r})}{\delta\mathbf{r}}=\mathbf{f}(\mathbf{r},t), \tag{1}$$

where μ is the mass density and γ is the dumping constant at a point $\mathbf{r}$. The vector $\mathbf{f}$ denotes the total contribution of external forces at $\mathbf{r}$ in an instant t. The term corresponding to the internal energy U, accumulated due to elastical deformation $\varepsilon(\mathbf{r})$, is estimated from the following empirical consideration

$$\epsilon(\mathbf{r})=\int_\Omega\sum_{i,j}(\Phi_{ij}(G_{ij}-G^0_{ij})^2+\Psi_{ij}(B_{ij}-B^0_{ij})^2)da_1da_2 \tag{2}$$

where $G_{ij}-G^0_{ij}$ and $B_{ij}-B^0_{ij}$ are, respectively, the variation of the metric and the curvature tensors with respect to its rest state, as detailed in Section 2, and Φ_{ij} and Ψ_{ij} are the elasticity constants. Roughly speaking, the metric tensors measure the variation of the area of the deforming surface and the curvature tensors give us the amount that a surface bends while it is deforming.

Instead of considering the deformable surface as a degenerated solid described in terms of a local Cartesian frame [6], the model proposed by Terzopoulos et al. embeds the surface displacements and normal vector variations in components described in terms of a Gaussian (intrinsic) frame. This approach explicits the variables that controls directly the local geometric behavior of the deforming surface.

In a previous work [8, 12], Ramos et al. noted that the model suffers from correct behavior under the resistance against bending. They conjectured that the problem came from the lack in the control of the relationship between the metric and curvature tensors while the surface is deforming. It is known that the metric and curvature tensors must satisfy certain compatibility differential equations known as Gauss formula and Mainardi-Codazzi equations [13, 3, 2]. However, from their tests, they concluded that, even when the compatibility equations are satisfied, unrealistic deforming behaviors concerning with bending may be yielded.

Attracted by the potential of the model in providing a more intuitive interface to the users, we decided to investigate more carefully the existing paradigms for implementing deformable surfaces on the basis of the local geometry properties. Our starting point is the classical shell theory, which regards a surface as a collection of points to each of which a vector out of a surface, called a *director*,

is assigned [7]. Its deformation is characterized by both the transformation of its coordinates as well as that of its directors. This surface is denominated Cosserat surface and presents the advantages that its formulation is performed in an analytic way, more appropriate for devising an interface that most of users are used to.

Simo and Fox [9, 10, 11] presented an efficient numerical implementation of the Cosserat surface, free from mathematical complexities such as the Christoffel symbols and the curvature tensors, in order to make it suitable for numerical analysis and finite element implementation. Modeling and control of fabrics has been benefited from their work [4, 6]. On the other hand, the implicitization of the geometric parameters, such as the curvature tensors, turns the relation between "what you control" and "what you see" more obscure.

Motivated by the user interface considerations, we present in this paper a novel proposal for a deformable model on the basis of the elastic Cosserat surface, maintaining all the components relative to a Gaussian (intrinsic) frame, such that we may define the dynamics of a surface shape through a set of constants called *deformation constants*, η, ξ and ϕ. Similar to the work of Terzopoulous et al., the constant η determines the amount that a surface stretches under the external forces and the constant ξ, how the surface bends. The new parameter ϕ controls the amount that the surface bends in each direction.

The paper is organized as follows. In section 2 some basic concepts of Differential Geometry are presented. We show the basis of the elastic Cosserat surface in section 3. Then, we present our proposal for modeling the kinematics of a deformable surface on the basis of the elastic Cosserat surface in section 4. Some simulation results is given in section 5 to illustrate the relationship between the specified elasticity parameters in our model and the obtained visual effects. Finally, in section 6 some concluding remarks are drawn.

2. Concepts

To be self-consistent some fundamental concepts necessary for understanding this paper are given.

Let $\mathbf{r}\colon \Omega \rightarrow R^3$ be a regular surface $\mathcal{S}$ [3] given by $\mathbf{r}(a_1, a_2) = (x(a_1, a_2), y(a_1, a_2), z(a_1, a_2))$, $a_1, a_2 \in \Omega$. As we have

$$d\mathbf{r} = \frac{\partial \mathbf{r}}{\partial a_1} da_1 + \frac{\partial \mathbf{r}}{\partial a_2} da_2, \tag{3}$$

the squared length $I(\mathbf{w})$ of an arc of a parameterized curve $\alpha(t) = \mathbf{r}(a_1(t), a_2(t))$, $t \in (-\delta, \delta)$, with $P = \alpha(0) = \mathbf{r}(a_1^0, a_2^0)$ and $\mathbf{w} = \alpha'(0)$, can be expressed by

$$\begin{aligned} I(\mathbf{w}) &= d\mathbf{r} \cdot d\mathbf{r} = \sum_{i,j=1}^{2} G_{ij} da_i da_j \\ &= \begin{bmatrix} da_i & da_j \end{bmatrix} \begin{bmatrix} G_{11} & G_{12} \\ G_{21} & G_{22} \end{bmatrix} \begin{bmatrix} da_i \\ da_j \end{bmatrix} \end{aligned} \tag{4}$$

where

$$G_{ij}(\mathbf{r}(a)) = \frac{\partial \mathbf{r}}{\partial a_i} \cdot \frac{\partial \mathbf{r}}{\partial a_j}. \tag{5}$$

The quadratic form, defined by Eq.(4), is the *first fundamental form* or *metric tensor* and their components G_{ij}, given by Eq.(4), are called the *metric*. Since the inner product is symmetric, we have $G_{12} = G_{21}$.

With the first fundamental form we can treat metric questions on a regular surface without further references to the ambient space R^3 where the surface lies. Therefore, all geometric properties expressed in terms of the metric coefficients, such as length, area, and angle, are invariant under isometries and are called *intrinsic* geometric properties.

The coefficients G^{ij} of the inverse matrix of the matrix given in Eq.(4) are

$$G^{11} = \frac{G_{22}}{G}, \;\; G^{12} = G^{21} = -\frac{G_{12}}{G}, \;\; G^{22} = \frac{G_{11}}{G}, \tag{6}$$

where

$$G = G_{11}G_{22} - G_{12}G_{21}. \tag{7}$$

The superscripts and subscripts denote, respectively, *contravariant* and *covariant* tensors. The difference between them is how they transform under a smooth change of coordinates. We denote G_0^{ij} the coefficients G^{ij} of the initial surface.

It can be shown that the *normal curvature* k_n of $\alpha(t) = \mathbf{r}(a_1(t), a_2(t))$ at the point $P = \alpha(0)$ with $\mathbf{w} = \alpha'(0)$ can be expressed as

$$II(\mathbf{w}) = k_n(\mathbf{w}) = \frac{\sum_{i,j=1}^{2} B_{ij} da_i da_j}{\sum_{i,j=1}^{2} G_{ij} da_i da_j}, \tag{8}$$

where

$$B_{ij} = \mathbf{n} \cdot \frac{\partial^2 \mathbf{r}}{\partial a_i \partial a_j} \tag{9}$$

with

$$\mathbf{n} = \left(\frac{\partial \mathbf{r}}{\partial a_1} \times \frac{\partial \mathbf{r}}{\partial a_2}\right) \Big/ \left\| \frac{\partial \mathbf{r}}{\partial a_1} \times \frac{\partial \mathbf{r}}{\partial a_2} \right\| \tag{10}$$

corresponding to the normal vector of $\mathcal{S}$ at P. The term

$$\sum_{i,j=1}^{2} B_{ij} da_i da_j = \begin{bmatrix} da_i & da_j \end{bmatrix} \begin{bmatrix} B_{11} & B_{12} \\ B_{21} & B_{22} \end{bmatrix} \begin{bmatrix} da_i \\ da_j \end{bmatrix} \tag{11}$$

is called the *second fundamental form* or *curvature tensor* and the elements B_{ij} are the *curvature coefficients*. The curvature coefficients are symmetric, that is, $B_{12} = B_{21}$.

The directions for which the normal curvatures (or the distances) is the minimum or maximum are called *curvature directions*. We call the normal curvatures in the curvature directions the *principal curvatures*, and denote them by k_1 and k_2.

In terms of the principal curvatures, we may define the *mean curvature*

$$H = \frac{k_1 + k_2}{2} = \frac{G_{11}B_{22} - 2G_{12}B_{12} + G_{22}B_{11}}{2(G_{11}G_{22} - G_{12}^2)} \quad (12)$$

and the *Gaussian curvature*

$$K = k_1 k_2 = \frac{B_{11}B_{22} - B_{12}^2}{(G_{11}G_{22} - G_{12}^2)}. \quad (13)$$

If $\mathcal{S}$ is orientable, it is possible to assign to each point a basis given by the vectors $\partial\mathbf{r}/\partial a_1$, $\partial\mathbf{r}/\partial a_2$ and $\mathbf{n}$. By expressing the derivatives of $\partial\mathbf{r}/\partial a_1$ and $\partial\mathbf{r}/\partial a_2$ in the basis $\partial\mathbf{r}/\partial a_1$, $\partial\mathbf{r}/\partial a_2$, $\mathbf{n}$, we obtain the Gauss formula

$$\frac{\partial^2\mathbf{r}}{\partial a_i \partial a_j} = \sum_{k=1}^{2} \Gamma_{ij}^k \frac{\partial\mathbf{r}}{\partial a_k} + B_{ij}\mathbf{n}, i, j = 1, 2, \quad (14)$$

where Γ_{ij}^k are the Christoffel symbols that depend exclusively on the coefficients of the first fundamental form and their derivatives as follows

$$\begin{aligned} \Gamma_{ij}^k &= \sum_{l=1}^{2} \frac{1}{2} G^{kl}\Big(\frac{\partial G_{jl}}{\partial a_i} + \frac{\partial G_{li}}{\partial a_j} - \frac{\partial G_{ij}}{\partial a_l}\Big) \\ &= \sum_{l=1}^{2} G^{kl}\Big(\frac{\partial^2\mathbf{r}}{\partial a_i \partial a_j} \cdot \frac{\partial\mathbf{r}}{\partial a_l}\Big). \end{aligned} \quad (15)$$

Hence, they are also intrinsic properties of $\mathcal{S}$ and all geometric concepts and properties expressed in terms of the Christoffel symbols are invariant under isometries. Since $\partial^2\mathbf{r}/\partial a_j a_i = \partial^2\mathbf{r}/\partial a_i a_j$, the Christoffel symbols are symmetric relative to the lower indices; that is, $\Gamma_{ij}^k = \Gamma_{ji}^k$.

The most surprising result is that all geometric properties expressed in terms of the Gaussian curvature K are *bending invariant*, that is, the properties that are unchanged by deformations which do not involve stretching, shrinking, or tearing. For example, a cylinder and a plane have the same Gaussian curvature. For distinguishing these two classes of shapes, we should use other measurements, such as the mean curvature H: the mean curvature of a plane is zero while that of a cylinder is nonzero. Unlike the Gaussian curvature, the mean curvature depends on the embedding and is closely related to the first variation of surface area.

When the intrinsic metric properties (distances of points along curvilinear coordinates or angles of their tangent directions at a point) change, the coefficients of the first and the second fundamental forms cannot vary independently. They should obey the Mainardi-Codazzi equations

$$\begin{aligned} \frac{\partial B_{11}}{\partial a_2} - \frac{\partial B_{12}}{\partial a_1} &= B_{11}\Gamma_{12}^1 + B_{12}(\Gamma_{12}^2 - \Gamma_{11}^1) - B_{22}\Gamma_{11}^2 \\ \frac{\partial B_{12}}{\partial a_2} - \frac{\partial B_{22}}{\partial a_1} &= B_{11}\Gamma_{22}^1 + B_{12}(\Gamma_{22}^2 - \Gamma_{12}^1) - B_{22}\Gamma_{12}^2 \end{aligned} \quad (16)$$

3. An elastic Cosserat Surface

A Cosserat surface is a surface that lies in the ambient space R^3, to evey point of which is assigned a vector pointing outwards the surface, called a *director*. The deformation of a Cosserat surface is characterized by both the basis vectors as well as that of its directors. The basis vectors provide the deformations of the intrinsic geometry of a surface while the directors may provide deformations that are not bending invariants. Figure 1 illustrates the change of the shape $\mathcal{S}_i$ of a deforming surface at time t_i to the shape $\mathcal{S}_{i+1}$ at time t_{i+1} by moving each point j along a direction $\mathbf{v}_j$ which results in a new set of points in 3D-space. The Theory of a Cosserat Surface ensures that this new set of points defines a regular surface, since a set of constitutive equations and the equation of balance of energy are satisfied [7].

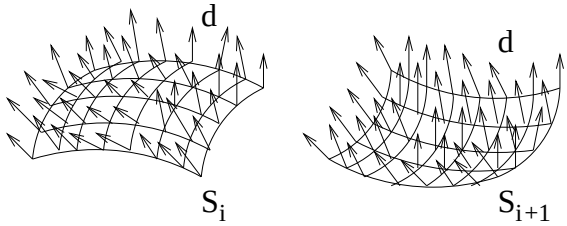

Figure 1. A Cosserat surface.

Let (x_1, x_2, x_3) refer to a fixed right-handed Cartesian coordinate system and t the time. Let (a_1, a_2, a_3) denote an arbitrary curvilinear coordinate system defined by the transformation

$$x_i = x_i(a_1, a_2, a_3, t), \quad det\Big[\frac{\partial x_i}{\partial a_j}\Big] > 0, \quad (17)$$

and its inverse. Let

$$\mathbf{r}(a_1, a_2, 0) = (x_1(a_1, a_2, 0), x_2(a_1, a_2, 0), x_3(a_1, a_2, 0)) \quad (18)$$

be a surface $\mathcal{S}$ that has two curvilinear coordinate curves, a_1- and a_2-curves, on it, and the third coordinate a_3 along

its normal $\mathbf{n}$. In the rest of this paper, we simply use $x_i(a_1, a_2)$ for referring $x_i(a_1, a_2, 0)$. Let $\mathbf{d}(t)$ be a director assigned to every point of $\mathcal{S}$. The motion of a Cosserat surface is characterized by

$$x_i = x_i(a_1, a_2, t), \quad \mathbf{d} = \mathbf{d}(a_1, a_2, t), \tag{19}$$

where $\mathbf{d}$ has the property that its components, referred to the base vectors $\{\frac{\partial \mathbf{r}}{\partial a_1}, \frac{\partial \mathbf{r}}{\partial a_2}, \mathbf{n}\}$, remain invariant when the motion is altered only by superposed rigid body motions.

Let σ, the area of $\mathcal{S}$ at time t, be bounded by a closed curve c and let ν be the outward unit normal to c lying in the surface. If $\mathbf{N}$ is a three-dimensional vector field and, if, for all arbitrary velocity fields $\mathbf{v}$, the scalar $\mathbf{N} \cdot \mathbf{v}$ represents a rate of work per unit length of c, then $\mathbf{N}$ is a *curve force vector* measured per unit length. Similarly, if $\mathbf{M}$ is a three-dimensional vector field and if, for all arbitrary director velocity fields $\mathbf{w}$, the scalar $\mathbf{M} \cdot \mathbf{w}$ represents a rate of work per unit length of c, then $\mathbf{M}$ is a *director force vector* measured per unit length. They may be expressed in terms of the base vectors a_i

$$\begin{aligned} \mathbf{N}^i &= \sum_{j=1}^{2} N^{ji} \frac{\partial \mathbf{r}}{\partial a_j} + N^{3i}\mathbf{n}, \quad i = 1, 2, \\ \mathbf{M}^i &= \sum_{j=1}^{2} M^{ji} \frac{\partial \mathbf{r}}{\partial a_j} + M^{3i}\mathbf{n}, \quad i = 1, 2, \end{aligned} \tag{20}$$

and transform as contravariant surface vectors. Thus, N^{ij} are surface tensors under transformation of surface coordinates.

Green et al. [7] showed that, with the assumption that the state of $\mathcal{S}$ remains unchanged under superposed uniform rigid body translational velocities, we may derive, from the equation of balance of energy, the equation of motion

$$\mu \frac{\partial^2 \mathbf{r}}{\partial t^2} - \sum_{i=1}^{2} \mathbf{N}^i|_i = \mathbf{f}(\mathbf{r}, t)\ , \tag{21}$$

where μ is the mass density and the vector $\mathbf{f}(\mathbf{r}, t)$ is the total contribution of external forces at $\mathbf{r}$ in an instant t. The term $\mathbf{N}^i|_i$ is the covariant derivative of $\mathbf{N}^i$ in relation to a_i at a point $\mathbf{r}$; that is

$$\mathbf{N}^i|_i = \frac{\partial \mathbf{N}^i}{\partial a_i} + \sum_j \Gamma^i_{ji} \mathbf{N}^j. \tag{22}$$

In addition, if $\mathbf{d} = \mathbf{n}$ at any instant t, the variables ε_{ij} and κ_{ij} that describe how the material behaves are given in terms of the variation of the coefficients of the first and the second fundamental forms, G_{ij} and B_{ij}, with respect to the (initial) undeformed state, G^0_{ij} and B^0_{ij}

$$\varepsilon_{ij} = \frac{1}{2}\Big(G_{ij} - G^0_{ij}\Big) \quad \text{and} \quad \kappa_{ij} = -\Big(B_{ij} - B^0_{ij}\Big). \tag{23}$$

For an elastic Cosserat surface which is anisotropic in its initial undeformed state and whose internal state is unaltered under uniform superposed rigid body angular velocities, Green et al. further derived the tensors $\mathbf{M}^{ij}$ and $\mathbf{N}^{*ij}$ in terms of the internal energy U

$$\begin{aligned} N^{*ij} &= \mu \frac{1}{2}\Big(\frac{\partial U}{\partial \varepsilon_{ij}} + \frac{\partial U}{\partial \varepsilon_{ji}}\Big) \\ M^{ij} &= \mu \frac{1}{2}\Big(\frac{\partial U}{\partial \kappa_{ij}} + \frac{\partial U}{\partial \kappa_{ji}}\Big). \end{aligned} \tag{24}$$

These tensors are related with the tensors N^{ij} in Eq.(20) through the expressions

$$N^{ij} = N^{*ij} - \sum_{k=1}^{2} B^i_k M^{jk} \quad \text{and} \quad N^{3j} = \sum_{k=1}^{2} M^{jk}|_k + \bar{L}^j, \tag{25}$$

where $M^{jk}|_k$ is the covariant derivative of M^{jk} with respect to the coordinate a_k, $\bar{\mathbf{L}}$ is the difference of the assigned director force per unit mass, $\mathbf{L}$, and the inertia terms due to the director displacement, and

$$B^i_j = \sum_{k=1}^{2} G^{ik} B_{jk}. \tag{26}$$

If the surface $\mathcal{S}$ is initially homogeneous, free from curve and director forces, and is at a constant temperature and entropy in the state of rest, then an approximation to the internal energy U may be written in the form

$$\mu_0 U = \sum_{i,j,k,l=1}^{2} \Big[A^{ijkl}\varepsilon_{ij}\varepsilon_{kl} + B^{ijkl}\kappa_{ij}\kappa_{kl} + C^{ijkl}\varepsilon_{ij}\kappa_{kl}\Big], \tag{27}$$

some of which satisfy certain symmetry conditions, if the elastic Cosserat surface possesses holohedral isotropy

$$\begin{aligned} A^{ijkl} &= A^{jikl} = A^{ijlk} = A^{klij} \\ &= \beta_1 G_0^{ij} G_0^{kl} + \beta_2 G_0^{ik} G_0^{jl} + \beta_3 G_0^{il} G_0^{jk} \\ B^{ijkl} &= B^{jikl} = B^{ijlk} = B^{klij} \\ &= \beta_4 G_0^{ij} G_0^{kl} + \beta_5 G_0^{ik} G_0^{jl} + \beta_6 G_0^{il} G_0^{jk} \\ C^{ijkl} &= C^{jikl} = C^{ijlk} = C^{klij} \\ &= \beta_7 G_0^{ij} G_0^{kl} + \beta_8 G_0^{ik} G_0^{jl} + \beta_9 G_0^{il} G_0^{jk}, \end{aligned} \tag{28}$$

once the holohedral isotropic materials are formed of crystalline substances having all faces symmetric; hence, their elastic properties are independent of the orientation of coordinate axes.

4. Our Proposal

From our exhaustive experimentations [8, 16], we observed that the simplified model proposed by Terzopoulos

et al. [14] cannot handle correctly the cases in which the intrinsic properties (length, angle, area, etc) change without affecting visually the curvature of the surface. More precisely, when the parameters Ψ_{ij} in Eq.(2) are different from zero, it is very difficult to obtain the expected behavior.

In [16], we presented the first proposal to improve the results generated by the model proposed by Terzopoulos et al. Our contribution was restricted to the implementation level: instead of approximating the normal vectors by the second derivatives, we used the Gauss formula to compute them. Larger range of satisfying visual effects was achieved. From the parameters Ψ_{ij}, we could easily differ the draping behavior of clothes from the behavior of card papers. However, we still had difficulties to specify behavior such as creases and folds. The question we posed was: although both are bending invariant (the Gaussian curvature is the same), what these two classes of behavior differ from?

A careful analysis led us to conclude that the two classes of bendings differ in the variation of the mean curvature and Eq.(12) shows us that the mean curvature depends on the mixed product of the coefficients of the first and the second fundamental form. It makes us to refer back to the existing theories for deforming surfaces to seek the one that takes the mixed terms into consideration.

We find these terms in Eq.(27) of the theory of elastic Cosserat surfaces. To simplify the expression, we further consider that the elastic material is holohedral isotropic. Although no material can be regarded as being holohedral isotropic in very small portions, the assumption of isotropy, when applied to an entire body, often does not lead to serious discrepancies between the experimental ans theoretical results. This lies in the fact that crystals are so small in comparison with the body and they are chaotically distributed in it that, in the large, the material behaves as though it were isotropic.

Since generally the contribution of the terms $C^{ijkl}\varepsilon_{ij}\kappa_{kl}$, $i,j \neq k,l$ is dominated by the contribution of the diagonal terms ($i = k$ and $j = l$), and aiming to a simple interface, we adopt the following simplified expression for computing the internal energy

$$\mu U = \sum_{i,j=1}^{2} \Big[\Phi^{ij}(\varepsilon_{ij})^2 + \Psi^{ij}(\kappa_{ij})^2 + \Theta^{ij}\varepsilon_{ij}\kappa_{ij}\Big], \quad (29)$$

where ε_{ij} and κ_{ij} are given in Eq.(23).

Comparing Eq.(29) with Eq.(2), one may note that they differ basically in the third term $\Theta^{ij}\varepsilon_{ij}\kappa_{kl}$. This term is fundamental for controlling behaviors that are bending invariant, such as folds and creases.

According to Eq.(28), the elasticity coefficients, Φ_{ij}, Ψ_{ij} and Θ_{ij}, are dependent on the metric tensor, which may vary while a surface is deforming. Again, in order to meet the tradeoff between the efficiency and the visual effects, we neglect the mixed terms in Eq.(28) which becomes

$$\begin{aligned} \Phi^{ij} &= \eta_{ij}\Big(2(G_0^{ij})^2 + G_0^{ii}G_0^{jj}\Big), \\ \Psi^{ij} &= \xi_{ij}\Big(2(G_0^{ij})^2 + G_0^{ii}G_0^{jj}\Big) \quad \text{and} \\ \Theta^{ij} &= \phi_{ij}\Big(2(G_0^{ij})^2 + G_0^{ii}G_0^{jj}\Big), \end{aligned} \quad (30)$$

where η_{ij}, ξ_{ij}, and ϕ_{ij} are referred as the *elasticity constants*. It is worth remarking that the elasticity constants in Eq.(2) are, in fact, particular cases of Eq.(30) in which the metric tensor at each point is $G_{ii}^0 = 1$ and $G_{12}^0 = G_{12}^0 = 0$. The most relevant difference that we observed in our experiments is that the constants supplied by the user, η_{ij}, ξ_{ij}, and ϕ_{ij}, tend to be invariant with respect to the mesh discretization (Section 5), while Φ_{ij}, Ψ_{ij} and Θ^{ij} must be adjusted for each chosen discretization step.

With the internal energy in hand, we may determine its corresponding elastic force. We further propose to substitute the term $\mathbf{N}^i|_i$ in Eq.(21) for $\frac{\delta\varepsilon(\mathbf{r})}{\delta\mathbf{r}}$ in Eq.(1), which yields

$$\mu\frac{\partial^2\mathbf{r}}{\partial t^2} + \lambda\frac{\partial\mathbf{r}}{\partial t} - \sum_{i=1}^{2}\mathbf{N}^i|_i = \mathbf{f}(\mathbf{r},t)\,. \quad (31)$$

The replacement leads to the explicit inclusion of geometric and physical restrictions, including the Mainardi-Codazzi compatibility equations (Eq.(16)), into the motion equation. The reason lies in the fact that $\mathbf{N}^i|_i$ depends on the Christoffel symbols and the components of the curve force vector, $\mathbf{N}^i$ (Eq.(22)). The components of $\mathbf{N}^i$ are, in their turn, dependent on the variation of the internal energy U with respect to the variation of the differential geometric properties of the deforming surface – the metric and the curvature tensors – from the rest state (Eqs.(24 and 25)). Thus, additional compatibility tests may be avoided.

Finally, we recall that the expression we proposed to be used for getting the internal energy U differs from the one used in the previous works [1, 5, 14]: Eq.(29) contains one more term $\Theta^{ij}\varepsilon_{ij}\kappa_{ij}$. We decompose $\mathbf{N}^i|_i$ into two components

$$-\sum_{i=1}^{2}\mathbf{N}^i|_i = \mathbf{l} + \mathbf{t}, \quad (32)$$

where $\mathbf{l}$ depends only on the term $\Theta^{ij}\varepsilon_{ij}\kappa_{ij}$ and $\mathbf{t}$ on the term $(\Phi^{ij}(\varepsilon_{ij})^2 + \Psi^{ij}(\kappa_{ij})^2)$ of the internal energy. This decomposition not only solves the singularity problem that we have when the rest state of the deforming surface is a plane (B_{ij}=0) but also let us to reduce the partial differential motion equations into a system of linked ordinary differential equations (Section 5). Replacing the sum in Eq.(31), we have as the motion equation

$$\mu\frac{\partial^2\mathbf{r}}{\partial t^2} + \lambda\frac{\partial\mathbf{r}}{\partial t} + \mathbf{t} = \mathbf{f}(\mathbf{r},t) - \mathbf{l}\,. \quad (33)$$

5. Simulation Results

Following the finite difference scheme proposed by Terzopoulos et al. [14], Eq.(33) is transformed into a system of linear equations. We should, however, assume that $\mathbf{l}$ is known in each iteration t_i. Our solution is, then, to use $\mathbf{l}$ of the iteration t_{i-1}. We believe that if the time step is sufficiently small, the errors should be acceptable for the visual purposes. Furthermore, the continuous space Ω is discretized into a $p \times q$-node mesh, where each node (k, l) represents a discrete point (or a *nodal variable*) $\mathbf{r}(k, l)$ in 3D space to which its normal is assigned as its director vector.

The values of $\mathbf{N}^{ij}$ at iteration t_i are computed from the differential geometric properties obtained at iteration t_{i-1}. We used the scheme presented in [16] for determining the normal vectors at each iteration. It is worth observing that Eq.(14) is only appliable in the cases where $B_{ij} \neq 0$. For overcoming this restriction, when $B_{ij} = 0$, we assume that the normal vectors do not change from the iteration t_{i-1} to t_i, that is, we use the normal vector of the iteration t_{i-1} in the iteration t_i computed by Eq. (10).

After some algebraic manipulations, we achieve the similar coupled system of differential equations as in [14] for each iteration t_i

$$M\frac{\partial^2 \mathcal{R}}{\partial t^2} + C\frac{\partial \mathcal{R}}{\partial t} + K(\mathbf{r})\mathcal{R} = \mathcal{F} - \mathcal{L} \qquad (34)$$

where

- M is the diagonal matrix formed by the mass density of each element,
- C, the diagonal matrix formed by the dumping density of each element,
- $K(\mathbf{r})\mathcal{R}$ corresponds to $\mathbf{t}$, where $K(\mathbf{r})$ is called the rigidity matrix,
- $\mathcal{F}$ is a column matrix containing the external force applied to each element, calculated from $\mathbf{f}(\mathbf{r}, t)$, and
- $\mathcal{L}$ is a column matrix containing the internal force $\mathbf{l}$ applied to each element at the iteration t_{i-1}.

Hence, the integration of the system through time for simulating the dynamics of a deforming surface may use the same step-by-step process presented in [14].

Eq.(30) shows that the material behavior of a deforming surface may be specified through three classes of *deformation constants*: η_{ij} for stretching, ξ_{ij} for bending, and ϕ_{ij} for the way the surface bends in the neighborhood of a point. Eqs.(29) and (31) tell us that the mass density, the damping density and the external forces should be provided. In our implementation, we simplified the interface by accepting the total mass m and the total damping factor c as input and the densities, μ and λ, are reevaluated according to the total area at time t

$$\mu_0 = \frac{m}{Area(\mathcal{S}(0))}, \quad \mu = \frac{Area(\mathcal{S}(0))}{Area(\mathcal{S}(t))}\mu_0$$
$$\lambda_0 = \frac{c}{Area(\mathcal{S}(0))}, \quad \lambda = \frac{Area(\mathcal{S}(t))}{Area(\mathcal{S}(0))}\lambda_0. \qquad (35)$$

In this section, we present some simulation results to illustrate and comment a few aspects related to the proposed model discussed so far. In the simulations presented, the initial shape is a plane, which is a singular case for our proposal.

(a) Photo

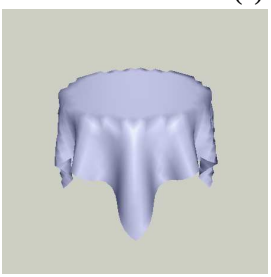

(b) without mixed terms

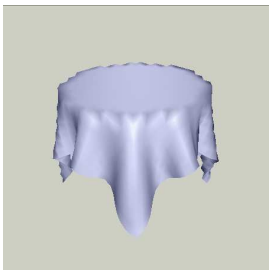

(c) with mixed terms

Figure 2. The draping of a cotton tablecloth.

In the first example we present the draping of a tablecloth 60×60 on a circular table. The discretization resolution used for the simulation was 31×31. The simulation parameters were: m = 738, c = 506.02, $\eta^{ii} = 30.5$, $\eta^{12} = \eta^{21} = 35.5$, $\xi^{ij} = 1.0$, $\phi^{ij} = 0.5$, the external force is the gravitational force, and all the nodes in contact with the table are fixed. For comparison purpose, Figure 2a shows a photo of a tablecloth and Figure 2b, the image generated from our proposed dynamics model. We believe that the almost realistic visual effect is due to the fact that the Mainardi-Codazzi equations are satisfied. In Figure 2c we include a result generated by a model that does not neglect the mixed terms in Eq.(28) for illustrating its similarity to the previous one.

To reinforce the importance of the Mainardi-Codazzi equations in governing the change of the coefficients of the first and the second fundamental forms, we present in Figure 3 the simulation of a waving flag (dimensions: 6.0×6.0)

whose two left vertices are fixed. The simulation parameters were: m=5.0, c=2.0, $\eta^{ij} = 8.0 \times 10^{-1}$, $\xi^{ij} = 1.0 \times 10^{-3}$, $\phi^{ij} = 1.0 \times 10^{-4}$, and the external force is the sum of [14]

$$\mathbf{f}_{fluid} = 0.032\Big[\mathbf{n} \cdot \Big(\mathbf{u} - \frac{\partial \mathbf{r}(a_1, a_2, t)}{\partial t}\Big)\Big]\mathbf{n}, \qquad (36)$$

where the constant stream velocity $\mathbf{u}$ is $(0, 3.0, 0)$, and a gravitational force

$$\mathbf{f}_{gravity} = \mu \mathbf{g}, \qquad (37)$$

with $\mathbf{g} = (-0.1, 0, 0)$. The discretization resolution was 15×15 in Figure 3a. It is interesting to note that if we increase the discretization resolution to 20×20, we may get similar visual effects with the same simulation parameters (Figure 3b).

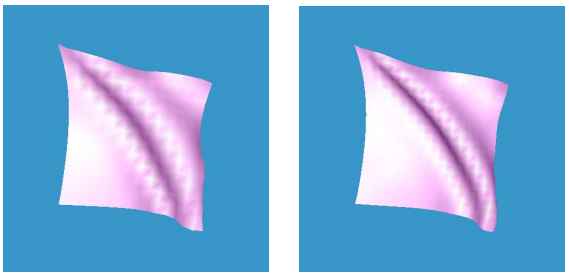

(a) 15×15 (b) 20×20

Figure 3. A waving flag.

For validating the efficiency of our model in simulating creases and folds, we present three more simulations.

Figure 4 aims to show the folds that we may create when we apply normal forces to the section of a shell, parallel to the curvilinear coordinate curves. Observe that the Gaussian curvature is maintained, while the mean curvature is increased. For allowing the variation of the normal curvatures in the vicinity of each point, ϕ_{ij} should be different from zero. In this particular case, the following simulation parameters were used: discretization resolution=20×20, m=5.0, c=3.0, $\eta^{ij} = 1.0$, $\xi^{i,j} = 5.0 \times 10^{-4}$, $\phi^{ij} = 1.0 \times 10^{-3}$, and the normal forces were applied on the nodes (4,4), (4,15), (15,4) and (15,15).

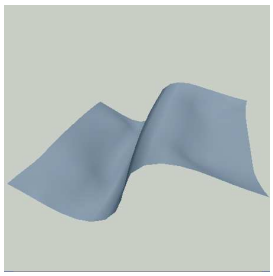

Figure 4. Folds due to the normal forces.

Figure 5 presents the simulation results for which we only changed the directions of the external forces: instead of being parallel to the curvilinear coordinate curves, they are from each vertex towards the center of the shell. Effects similar to the creases are generated.

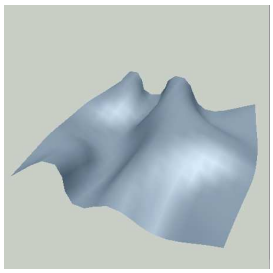

Figure 5. Creases.

Finally, we show in Figure 6b the simulation of a cotton handkerchief (dimensions: 60×60) hanging on a point. Only the gravitational force acts in it. The simulation parameters were: discretization resolution = 30×30, m=737.4, c=220.0, $\eta^{ii} = 190.5$, $\eta^{12} = \eta 21 = 220.5$, $\xi^{ij} = 1.0 \times 10^{-4}$, and $\phi^{ij} = 1.0 \times 10^{-4}$. A photo of a real situation is included for comparison.

6. Concluding Remarks

We present a deformation model on the basis of the theory of the Cosserat surface. In comparison with the well-known physically-based deformation model proposed by Terzopoulos et al., our model has the same strong geometric appeal and

1. presents one more term in the expression of the internal energy, providing a direct way to specify how a surface should bend in the neighborhood of each point on the surface, in order to model more naturally the foldings and the creases;

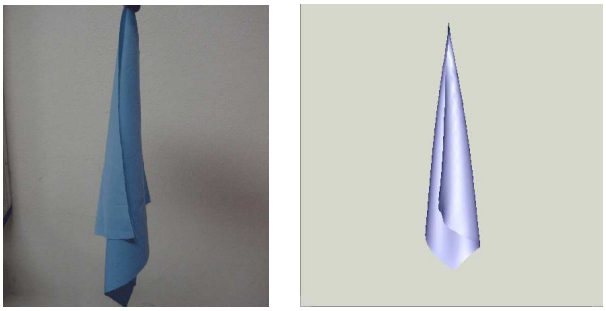

(a) Photo (b) Simulation

Figure 6. A hanging handkerchief.

2. ensures the geometrical compatibility, providing more realistic visual effects; and

3. presents a set of elasticity constants that are invariant with respect to the discretization resolution, providing more intuitive interface to its users.

However, our simulations present problems concerning with the boundary conditions of the method of finite differences we used. In the way that we implemented the finite differences, the first and the second derivatives are not completely defined in two edges of the border of the domain Ω. This may cause unexpected visual effects as illustrates Figure 7. Observe that two opposite extremes of the tablecloth crease in a unrealistic way, while the other two opposite extremes present a realistic behavior. The extremes that crease unnaturally belong to the edges whose boundary conditions are not well-defined.

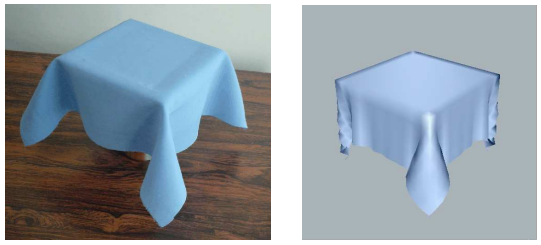

(a) Photo (b) Simulation

Figure 7. A square tablecloth.

Additionally, to make our model effectively applicable we should integrate an efficient algorithm of handling collisions and self-intersections. This will leave as further work.

7. Acknowledgment

The second author also aknowledge UFCG for the support to his work at Unicamp in the context of the PICD/CAPES Program.

References

[1] C. K. Au, Z. Wu, and M. M. F. Yuen. Effect of fabric properties on cloth draping modeling. In *Proceedings IEEE Conf. on Geometric Modeling and Processing 2000*, pages 69–76, Hong Kong, 2000.

[2] M. Berger and B. Gostiaux. *Differential Geometry: Manifolds, Curves and Surfaces*. Springer-Verlag, New York, 1988.

[3] M. P. Carmo. *Differential Geometry of Curves and Surfaces*. Prentice Hall Englewood Cliffs, N.J., 1976.

[4] B. Chen and M. Govindaraj. A physically based model of fabric drape using flexible shell theory. *Textile Research Journal*, 65(6):324–330, 1995.

[5] J. Eischen and Bigliani. Continuum versus particle representations. In D. House and D. Breen, editors, *Cloth Modeling and Animation*, pages 79–122. A. K. Peters, 2000.

[6] J. W. Eischen, S. Deng, and T. G. Clapp. Finite-element modeling and control of flexible fabric parts. *IEEE Computer Graphics and Applications*, pages 71–80, 1996.

[7] A. E. Green, P. M. Naghdi, and W. L. Wainwrigh. A general theory of a cosserat surface. *Arch. Rat. Mech. An.*, 20:287–308, 1965.

[8] P. S. C. Ramos and S. T. Wu. Analyzing a deformable model using differential geometry. In *Proceedings of X SIBGRAPI*, pages 57–64. IEEE - Computer Society, 1997.

[9] J. C. Simo and D. D. Fox. On a stress resultant geometrically exact shell model. part i: Formulation and optimal parameterization. *Computer Methods in Applied Mechanics and Engeneering*, 72:267–304., 1989.

[10] J. C. Simo and D. D. Fox. On a stress resultant geometrically exact shell model. part ii: The linear theory; computational aspects. *Computer Methods in Applied Mechanics and Engeneering*, 73:53–92, 1989.

[11] J. C. Simo and D. D. Fox. On a stress resultant geometrically exact shell model. part iii: Aspects of the nonlinear theory. *Computer Methods in Applied Mechanics and Engeneering*, 79:21–70, 1989.

[12] Site. http://www.dca.fee.unicamp.br/projects/desmo/.

[13] D. J. Struik. *Lectures on Classical Differential Geometry*. Addison-Wesley Publishing Co., London, 1961.

[14] D. Terzopoulos, P. J., B. A., and F. K. Elastically deformable models. *Computer Graphics*, 20(4):205–214, 1987.

[15] J. Weil. The synthesis of cloth objects. *Computer Graphics*, 20(4):49–54, 1986.

[16] S. T. Wu and V. F. Melo. An approximation for normal vectors of deformable models. In *Proceedings of SIBGRAPI '2003*, pages 3–10. IEEE - Computer Society, 2003.